Innovative: International Multi-disciplinary Journal of Applied Technology
(ISSN 2995-486X) VOLUME 02 ISSUE 03, 2024

Development the Adhesion and Antibacterial Properties of the Centrifuge Device

Abdul Rahman Ali Rahim
Medical device engineering, Al-Israa University College
Ali Hussein Falih
Medical device engineering, Al-Israa University College
Amir Jassim Muhammad
Medical device engineering, Al-Israa University College

Abstract:

The fabrication of antibacterial surfaces that exhibit enhanced activity toward a large variety of bacteria species is one of the major challenges of our time. ZnO NPs have become one of the most popular metal oxide nanoparticles in biological applications due to their excellent.

biocompatibility, economic, and low toxicity, and have emerged a promising potential in biomedicine, especially in the fields of anticancer and antibacterial fields, In this work, The anti-bacterial and adhesion properties of the centrifuge rotor will be improved by the use of zinc oxide as an anti-bacterial material and using coating to reduce the adhesion.

Keywords: adhesion, antibacterial properties, biocompatibility, economic

Introduction

Nanomaterial's display unique, superior and indispensable properties and have attracted much attention for their distinct characteristics that are unavailable in conventional macroscopic materials. Their uniqueness arises specifically from higher surface to volume ratio and increased percentage of materials in the development of novel devices that can be used in various physical, biological, biomedical and pharmaceutical applications [1]. Due to the reduced size of their constituent elements nanostructured materials have electronic, magnetic and chemical properties, which differ

considerably from those of the corresponding bulk materials. For example, nanostructured materials have been found to exhibit increased strength and hardness, higher electrical resistivity, enhanced diffusivity, reduced density, etc. compared to the bulk due to quantum confinement effect [2]. Hence, these materials are promising candidates for a variety of applications, which include heterogeneous catalysis, gas sensor technology, microelectronics, nonlinear optics, etc. [3]. Discoveries have led to the observation that new properties exist when the size of materials is on the Nano scale due to electronic confinement in semi-conductors and surface effects in metals. The significance of Nano scale quantum confinement of the electrons provides visualization of the shift in the characteristics of the material depending on the size of the nanoparticles [4]. Noble metal nanoparticles such as Ag and Au NPs have been a source of great interest due to their novel electrical, optical, physical, chemical and magnetic properties [5].The main characteristics of metallic NPs are large surface energies, specific electronic structure, Plasmon excitation and quantum confinement [6].Moreover, silver nanoparticles are being used in numerous technologies such as; desirable optical, conductive, and antibacterial properties. These applications can be categorized to diagnostic applications, conductive applications, optical

applications and antibacterial applications [7].Silver is a nontoxic, safe inorganic antibacterial agent capable of killing about 650 types of diseases causing microorganisms. Silver has ability to exert a bactericidal effect at minute concentrations. It has a significant potential for a wide range of biological applications such as antibacterial agents for antibiotic resistant bacteria, preventing infections [8]. Previous studies [7- 9-10] have proposed three mechanisms of the antimicrobial activities of Ag-NPs: (i) Could attach to cell membrane and disrupt the permeability and respiration functions of the cell and thus kill the cells; (ii) Reactive oxygen species (ROS) can be generated on the surface of nanoparticles and cause damage of DNA by exerting oxidative stress; (iii) Silver ions released from Ag-NP's can also cause disruption of ATP production and DNA replication. These Nano-materials have been used as sterile materials that kill bacteria, and their actions have been applied to the Centrifuge device. Where we used as a coating to kill the bacteria on the surface of the device. The Aim of this work In this work, the anti-bacterial and adhesion properties of the centrifuge rotor will be improved by the use of nanoparticles like zinc oxide as an anti-bacterial material and using coating to reduce the adhesionSilver nanoparticles are nanoparticles of silver of between 1 nm and 100 nm in size.[1] While frequently described as being 'silver' some are composed of a large percentage of silver oxide due to their large ratio of surface to bulk silver atoms. Numerous shapes of nanoparticles can be constructed depending on the application at hand. Commonly used silver nanoparticles are spherical, but diamond, octagonal, and thin sheets are also common [11]. The Nano-technology is rapidly growing technology with an enormous potential to develop materials and enhanced products for many applications with unique properties. Many Nano-based products are already pierced into marketplaces; include personal care, electronics device, medical instruments, and sporting goods. Despite, there is attention around the influence of the "Nano-materials" on both "human health" and the environment. Recognizing and understanding the potential risks that may be correlated with the usage of the "Nano-materials" is a critical step if these materials are to be dominating future applications [12]. One of most "crucial things" to determine special definition: nanostructure, which defines as any structure (cluster, molecule, and crystallites) with one or more "dimensions measuring" in range less than 100 m, placing it as intermediate in size between the "molecule and bacterium". The definition modifies further this, stating that nanostructure should have the characteristic

dimension vary between 1nm and 100 nm [13].Seed-mediated growth is a synthetic method in which small, stable nuclei are grown in a separate chemical environment to a desired size and shape. Seedmediated methods consist of two different stages: nucleation and growth. Variation of certain factors in the synthesis (e.g. ligand, nucleation time, reducing agent, etc.), [14] can control the final size and shape of nanoparticles, making seedmediated growth a popular synthetic approach to controlling morphology of nanoparticles. The nucleation stage of seed-mediated growth consists of the reduction of metal ions in a precursor to metal atoms. In order to control the size distribution of the seeds, the period of nucleation should be made short for monodispersity. The LaMer model illustrates this concept [15]. Seeds typically consist small nanoparticles, stabilized by a ligand. Ligands are small, usually organic molecules that bind to the surface of particles, preventing seeds from further growth. Ligands are necessary as they increase the energy barrier of coagulation, preventing agglomeration. The balance between attractive and repulsive forces within colloidal solutions can be modeled by DLVO theory [16].

Although silver nanoparticles are widely used in a variety of commercial products, there has only recently been a major effort to study their effects on human health. There have been several studies that describe the in vitro toxicity of silver nanoparticles to a variety of different organs, including the lung, liver, skin, brain, and reproductive organs.[17] The mechanism of the toxicity of silver nanoparticles to human cells appears to be derived from oxidative stress and inflammation that is caused by the generation of reactive oxygen species (ROS) stimulated by either the Ag NPs, Ag ions, or both [18].

Top-down and bottom-up are two approaches for the manufacture of products.

These terms were first applied to the field of nanotechnology by the Foresight Institute in 1989 in order to distinguish between molecular manufacturing (to mass-produce large atomically precise objects) and conventional manufacturing (which can mass-produce large objects that are not atomically precise).

Bottom-up approaches seek to have smaller (usually molecular) components built up into more complex assemblies, while top-down approaches seek to create Nanoscale devices by using larger, externally controlled ones to direct their assembly. Certain valuable nanostructures, such as Silicon nanowires, can be fabricated using either approach, with processing methods selected on the basis of targeted applications.

The top-down approach often uses the traditional workshop or Micro-fabrication methods where externally controlled tools are used to cut, mill, and shape materials into the desired shape and order. Micro-patterning techniques, such as photolithography and inkjet printing belong to this category. Vapor treatment can be regarded as new top-down secondary approaches to engineer nanostructures [91].

Bottom-up approaches, in contrast, use the chemical properties of single molecules to cause single-molecule components to (a) self-organize or self-assemble into some useful conformation, or (b) rely on positional assembly. These approaches utilize the concepts of molecular self-assembly and/or molecular recognition.

Such bottom-up approaches should, broadly speaking, be able to produce devices in parallel and much cheaper than top-down methods, but could potentially be overwhelmed as the size and complexity of the desired assembly increases.

The medical uses of silver include its use in wound dressings, creams, and as an antibiotic coating on medical devices. Wound dressings containing silver sulfadiazine or silver Nano-materials may be used to treat external infections. The limited evidence available shows that silver coatings on endotracheal breathing tubes may reduce the incidence of ventilator-associated pneumonia [20]. There is tentative evidence that using silver-alloy indwelling catheters for short-term catheterizing will reduce the risk of catheter-acquired urinary tract infections.

Silver generally has low toxicity, and minimal risk is expected when silver is used in approved medical applications. Alternative medicine products such as colloidal silver are not safe or effective [21].

Silver sulfadiazine (SSD) is a topical antibiotic used in partial thickness and full thickness burns to prevent infection it was discovered in the 1960s, and was the standard topical antimicrobial for burn wounds for decades.

However systemic reviews in 2014, 2017 and 2018 concluded that more modern treatments, both with and without silver, show better results for wound healing and infection-prevention than silver sulfadiazine, and therefore SSD is no longer generally recommended [22].

It is on the World Health Organization's List of Essential Medicines, the safest and most effective medicines needed in a health system. The US Food and Drug Administration (FDA) approved a number of topical preparations of silver sulfadiazine for treatment of second-degree and third-degree burns [23]. A 2018 Cochrane review found that silver-containing dressings may increase the probability of healing for venous leg ulcers. A 2017 meta-analysis of clinical studies over the period of 2000-2015 concluded that "the evidence base for silver in wound management is significantly better than perceived in the current scientific debate" and that, if applied selectively and for short periods of time, silver has antimicrobial effects, produces an improvement in quality of life and shows good cost-effectiveness [24]. A 2014 data set from a recent meta-analysis concluded that the use of silver dressings improves healing time, and can lead to overall cost savings compared with treatment with non-silver dressings. A 2015 systematic review concluded that the limited evidence available indicates that using silver-coated endotracheal breathing tubes reduces the risk of contracting ventilator-associated pneumonia (VAP), especially during the initial days of utilization. A 2014 study concluded that using silver-coated endotracheal tubes will help to prevent VAP and that this may save on hospital costs. A 2012 systematic review of randomized controlled trials concluded that the limited evidence available indicates that using silver-coated endotracheal tubes will reduce the incidence of ventilator-associated pneumonia, microbiologic burden, and device-related adverse events among adult patients [25]. A 2014 systemic review concluded that using silver alloy-coated catheters showed no significant difference in incidences of symptomatic Catheter-Associated Urinary Tract Infections (CAUTI) versus using standard catheters, although silveralloy catheters seemed to cause less discomfort to patients. These catheters are associated with greater cost than other catheters [26]. A 2014 Multicenter Cohort Study found that using a silver-alloy hydrogel urinary catheter did reduce symptomatic Catheter-Associated Urinary Tract Infection (CAUTI) occurrences as defined by both

NHSN and clinical criteria. Research in 2018 into the treatment of central nervous system infections caused by free-living amoebae such as Naegleria fowleri and Acanthamoeba castellanii, tested the effectiveness of existing drugs as well as the effectiveness of the same drugs when they were conjugated with silver nanoparticles. In vitro tests demonstrated more potent amoebicidal effects for the drugs when conjugated with silver nanoparticles as compared to the same drugs when used alone. They also found that conjugating the drugs with silver nanoparticles enhanced their antiacanthamoebic activity [27]. Silver-halide imaging plates used with X-ray imaging were the standard before digital techniques arrived; these functions essentially the same as other silverhalide photographic films, although for x-ray use the developing process is very simple and takes only a few minutes. Silver x-ray film remains popular for its accuracy, and cost effectiveness, particularly in developing countries, where digital X-ray technology is usually not available [28]. Other uses of silver compounds have been used in external preparations as antiseptics, including both silver nitrate and silver proteinase, which can be used in dilute solution as eye drops to prevent conjunctivitis in newborn babies. Silver nitrate is also sometimes used in dermatology in solid stick form as a caustic ("lunar caustic") to treat certain skin conditions, such as corns and warts [29]. Silver nitrate is also used in certain laboratory procedures to stain cells. As it turns them permanently a dark-purple/black color, in doing so increasing individual cells' visibility under a microscope and allowing for differentiation between cells, or identification of irregularities. Bacteria are a type of biological cell. They constitute a large domain of prokaryotic microorganisms. Typically, a few micrometers in length, bacteria have a number of shapes, ranging from spheres to rods and spirals. Bacteria were among the first life forms to appear on Earth, and are present in most of its habitats. Bacteria inhabit soil, water, acidic hot springs, radioactive waste, and the deep biosphere of the earth's crust. Bacteria also live in symbiotic and parasitic relationships with plants and animals. Most bacteria have not been characterized, and only about 27 percent of the bacterial phyla have species that can be grown in the laboratory The study of bacteria is known as bacteriology, a branch of microbiology.

Nearly all animal life is dependent on bacteria for survival as only bacteria and some archaic possess the genes and enzymes necessary to synthesize vitamin B12, also known as cobalamin, and provide it through the food chain. Vitamin B12 is a water-soluble vitamin that is involved in the metabolism of every cell of the human body. It is a cofactor in DNA synthesis, and in both fatty acid and amino acid metabolism [30]. Many bacterial species exist simply as single cells, others associate in characteristic patterns: Neisseria form diploids (pairs), Streptococcus form chains, and Staphylococcus group together in "bunch of grapes" clusters. Bacteria can also group to form larger multicellular structures, such as the elongated filaments of Actinobacteria, the aggregates of Myxobacteria, and the complex hyphae of Streptomyces. These multicellular structures are often only seen in certain conditions. For example, when starved of amino acids, Myxobacteria detect surrounding cells in a process known as quorum sensing, migrate towards each other, and aggregate to form fruiting bodies up to 500 micrometers long and containing approximately 100,000 bacterial.

Bacteria often attach to surfaces and form dense aggregations called biofilms, and larger formations known as microbial mats. These biofilms and mats can range from a few micrometers in thickness to up to half a meter in depth, and may contain multiple species of bacteria, protists and archaea. Bacteria living in biofilms display a complex arrangement of cells and extracellular components, forming secondary structures, such as micro colonies, through which there are networks of channels to enable better diffusion of nutrients. In natural environments, such as soil or the surfaces of plants, the

majority of bacteria are bound to surfaces in biofilms .Biofilms are also important in medicine, as these structures are often present during chronic bacterial infections or in infections of implanted medical devices, and bacteria protected within biofilms are much harder to kill than individual isolated bacteria [31-37].

3.Experimental work (Methodology):

In this study will be dealing with experimental part and includes preparation of un doped and Zn(NO_3) nanostructure doped with Ag(NO_3), Fe_2 (No_3),and Cu(NO_3) using inexpensive, simple low-cost chemical precipitation method at different conditions. Subsequently, the products doped ZnO nanostructure modifying using SA with different molar ratios, following by the deposition of ZnO on a glass substrate using a drop casting method. Also doped ZnO nanostructure will mix with PVC polymer at different ratios of solvent\non solvent to obtain antibacterial and super-hydrophobicicty property at same surface. And finally, studying antibacterial activity of Ag(NO_3), Fe_2 (No_3),and Cu(NO_3) doped ZnO/PVC Nano-composite.

Doped ZnO Synthesis Fabrication of Zn doped ZnO nanostructures:

In typical manufacturing, 1 g concentration of Zn (NO_3) was suspended or dissolved in 20 ml of distilled water after magnetic support and stirring for 60 minutes to obtain a homogeneous solution. Then 1 M of NaOH was added drop wise into the above solution to obtain the precipitate while stirring. Continuous magnetism and a certain temperature showed a milky color to the processed solution; left overnight and then the sediment is collected by centrifugation after rinsing with distilled water and ethanol for excellent cleaning. After that, the precipitate obtained by the oven is dried at a temperature of 100 degrees C for 6 h and then completely grounded The finely precipitated powder undergoes heat treatment at 300 ° C to 3 hours to achieve Zn-doped ZnO powder

Fabrication of Ag doped ZnO nanostructures:

In a typical composition, 1 gram of Ag (No3) was suspended or dissolved in 20 mL of distilled water after supportive magnetic stirring for 60 min to obtain a homogeneous solution and then Zn (NO3) was added with continued magnetic stirring and heat Dark brown color. Then 3 M of sodium hydroxide was added. sodium hydroxide was distilled into the above solution with continuous stirring to obtain the obtained precipitate .

Structural and morphological studies

X-Ray Diffraction (XRD):

Doped ZnO nanostructures crystalline phase were analyzed by XRD instrumentation at room temperature by using "Miniflex II Rigaku, Japan" provided with Cu tube for producing Cuk_α radiation (λ= 1.5408Å). The incident beam in the 2Θ mode overhead the range of (10^o – 80^o), and worked by (30 kV) voltage and (40 mA) filament current. The data of Specimens in this work was done via matching the intensities and positions of element peak in XRD patterns to those patterns in the database of JCPDS (Joint Committee on Powder Diffraction Standards).

XRD measurement carried out in the College Of Education Ibn alHaytham / Baghdad University.

Field Emission Scanning Electron Microscopy (FESEM):

All specimens were studied through FESEM-EDX (Hitachi-S 4160- Japan) in CAC center of research "Iran" and need to be capable to stand the powerful "electric-currents" which generated by using electron beam gun. Any non-conductive specimens can be destroyed due to the build-up of charges on surfaces. Therefore, the coated of non-conductive specimens with the thin layer of conductive-material e.g. gold by using a small sputtering system leads to avoid this problem.

Antimicrobial activity test:

The antimicrobial performance of Ag, Fe_2O_3, and Ag-Fe_2O_3doped ZnO/PVC nano-composite have been examined against bacterial cultures Gram positive bacteria Staphylococcus epidermidis (staph. epidermidis) and Gram negative bacteria Klebsiella pneumoniae (Klebsiella spp.). We have opted these two different kinds of pathogenic microbes because of the following reasons:-

► Staph. Epidermidis: Gram-positive bacteria causes biofilms to grow on "plastic devices" fixed inside the body. This occurs most usually on intravenous medical prostheses and catheters. The infection can similarly occur in "dialysis patients" or anyone with an implanted plastic. In remarkable other cases, sepsis can happen in "hospital patients".

► Klebsiella Spp.: Gram-negative bacteria causes a wide range of disease states, urinary tract infections, very pneumonia, meningitis, sepsis, soft tissue infections, and diarrhea; also most infections include infection of an invasive medical device.

4. *Result and discussion*

The present chapterincludes experimental results and analysis of (Ag, Fe) nanoparticles and doped on ZnO structure sample prepared by seed growth technique by using a simple chemical precipitation method, with discussing the results.

The various characteristics like optical, electrical rely on structure or morphology of Nano-particles therefore the structure and morphology characteristics are regarded very indispensable merits. Numerous methods are utilized according to investigation of the structural properties for example XRD- X-ray diffraction, FESEM- Field Emission Scanning Electron Microscope.

XRD and EDX measurements:

XRD is a vigorous technique utilized because of finding out the crystal structure of crystalline material by means of a diffraction test sample or for measuring the structure properties like (strain state, grain size, and distinguish orientation) about it phases, and it's non-damaging and doesn't need any elaboration setup.

Ag doped ZnO nanostructures:

Figure 4-1 (a,b) displays the XRD spectra of un doped ZnO and Ag-doped ZnO nanostructures prepare by a co-precipitation method, with diffraction peaks confirm appeared ZnO with quartzite hexagonal phase and polycrystalline structure. For ZnO All diffraction peaks in the XRD spectra corresponding to the (101), (002), (100), (102), (103), (110), (112), (200), and (201) miller indices; For Ag, the diffraction peaks of the XRD spectra corresponding to (111) (200) miller indices as illustrated in a table (4-1).

The higher peak intensities of XRD spectra are due to the high crystallinity. From this figure, it is clear that the spectra of X-ray diffraction have sharp and very fine peaks. It means that the ZnO is polycrystalline with hexagonal and the major peak is in the direction (101) with high intensity show the dominate growth direction. Table (4.2) is shown the grain size of Ag doped ZnO nanostructures.

In figure 4-1 (b), none distinct peaks of Ag within the spectra of XRD indicating that homogeneously distributed of Ag particles in the zinc matrix. With the insert Ag in ZnO structure, the change in FWHM values and shifting in position observed as compared with un doped ZnO, which indicates that structural changes occur after Ag doped ZnO.

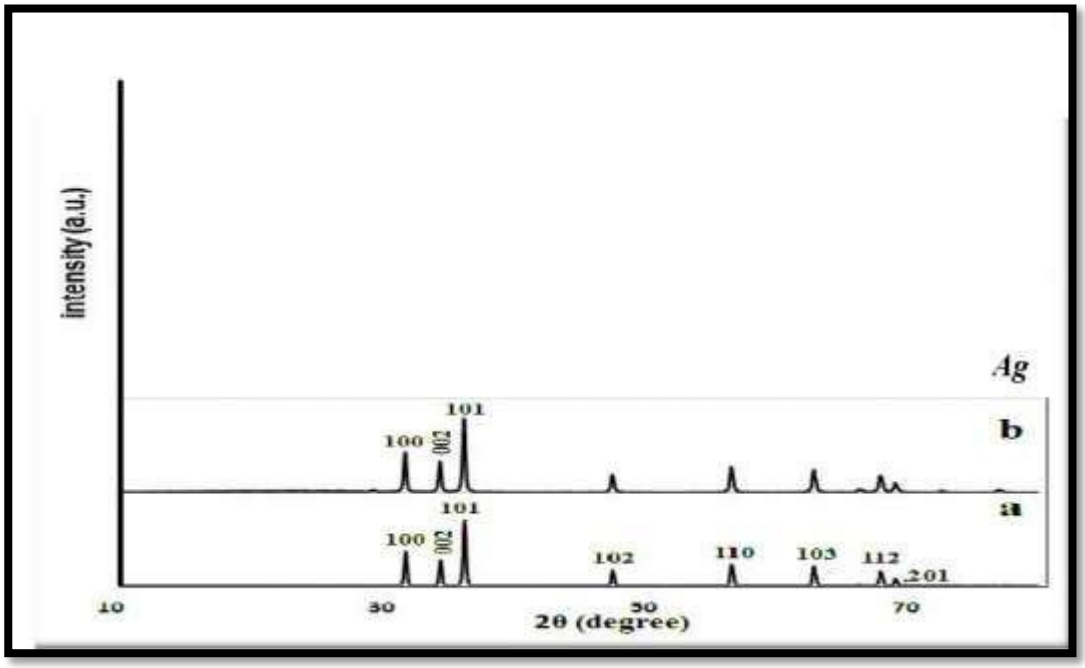

Figure (1): XRD pattern of (a) un doped ZnO and (b) Ag doped ZnO

nanostructures at concentrations 1%.

Figure (2) depicts the EDX spectra of un doped ZnO and Ag-doped ZnO. From this figure, the results prove that the synthesized undoped ZnO specimen principally includes elements of Zinc(Zn), Carbon (C), and Oxygen (O); With a peak of C appears at 0.02 keV and a peak of O appear at 0.5 keV while Zn appears at peaks of 9.5 keV, 8.6 keV, and 1 keV, as shown during figure 4-2 (a).

No traces of other elements were observed in the spectra, which prove the purity of the specimen. However, in figure 4-2 (b) EDX spectra indicate that the synthesize Ag-doped ZnO specimen principally includes Ag, Zn, C, and O elements; With a peak of Ag appears at 3 Kev, C appears at 0.02 keV and a peak of O appear at

0.5keV; while Zn appears at peaks of 9.5keV, 8.6keV, and 1 keV.

Accordingly, EDX results are agreeable with the XRD result of undoped and Agdoped ZnO pecimens.

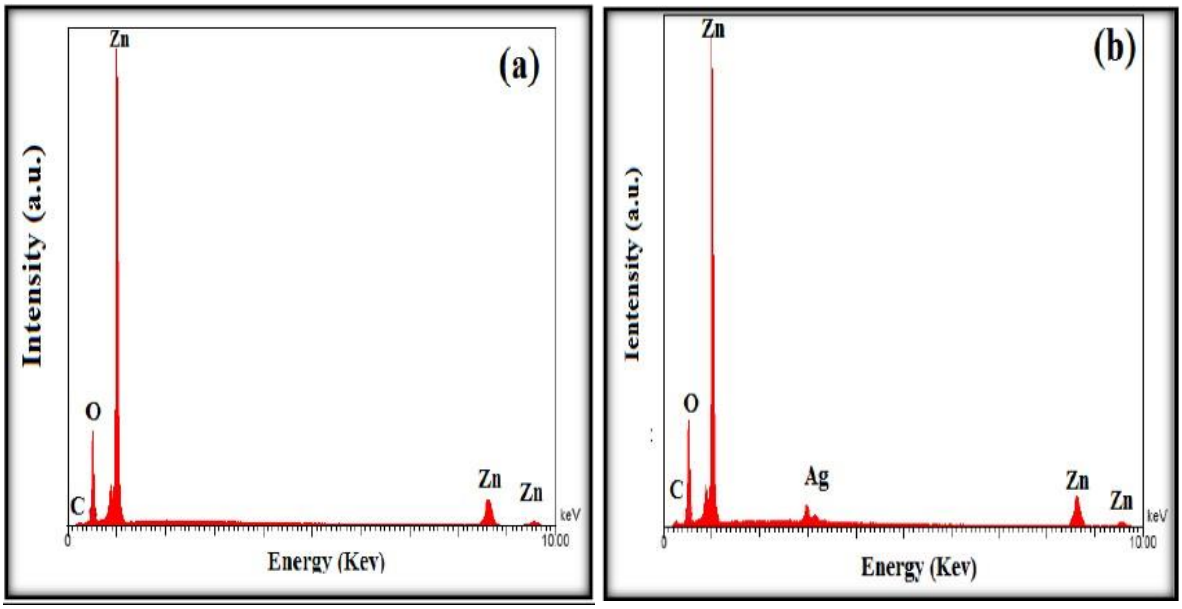

Figure (2): EDX spectrum of (a) undoped ZnO and (b) Ag doped ZnO nanostructures.

Table (1): XRD results of Ag doped ZnO nanostructures.

Prepared conditions	*(2Θ)° XRD*	***I/Io** XRD*	*d(Å) XRD*	*(h k l)*	*FWHM XRD*	*(2Θ)° JCPDS*
Un doped ZnO	31.47	64	2.84224	(100)	0.249	31.76
	34.10	45	2.62696	(002)	0.243	34.42
	35.96	100	2.49722	(101)	0.264	36.25

	47.22 56.27 62.53 67.62 68.76	20 33 27 21 13	1.92311 1.63353 1.48402 1.38421 1.36411	(102) (110) (103) (112) (201)	0.279 0.258 0.259 0.282 0.183	47.53 56.60 62.86 67.96 69.09
1% Ag doped ZnO	31.38 34.48 36.31 47.59 56.64 62.90 67.99 69.13	53 40 100 25 39 35 27 14	2.80910 2.61981 2.47208 1.90913 1.62367 1.47617 1.37761 1.35764	(100) (002) (101) (102) (110) (103) (112) (201)	0.227 0.227 0.223 0.235 0.226 0.230 0.246 0.240	- - - - - - - -

Table (2): Structural parameters of Ag doped ZnO nanostructures.

Prepared conditions	*(h k l)*	*D (nm)*
Un doped ZnO	(101)	30.1

1% Ag doped ZnO	(101)	37.40

4.2.1.2 Fe_2O_3 doped ZnO Nanostructures:

Figure 4-3 (a-b) reveals to XRD spectra of un doped and Fe_2O_3 doped ZnO nanostructures with diffraction peaks prove to appear a hexagonal phase and polycrystalline structure of ZnO. For ZnO all diffraction peaks in the XRD patterns corresponding to the (101), (002), (100),(102),(103),(110),(112),(200), and (201) miller indices. Concerning Fe_2O_3 the diffraction peaks within the XRD spectra corresponding to (220) (006) (202) miller indices as illustrated in a table (3). From this figure, it is clear that the spectra of X-ray diffraction have sharp and very fine peaks indicate good crystallization. Table (3) is shown the grain size of Fe_2O_3 doped ZnO nanostructures.

With the insert Fe_2O_3 in ZnO structure, we observed change in FWHM values and shifting in position as compared with un doped ZnO, which indicates that structural changes occur after Fe_2O_3 doped ZnO.

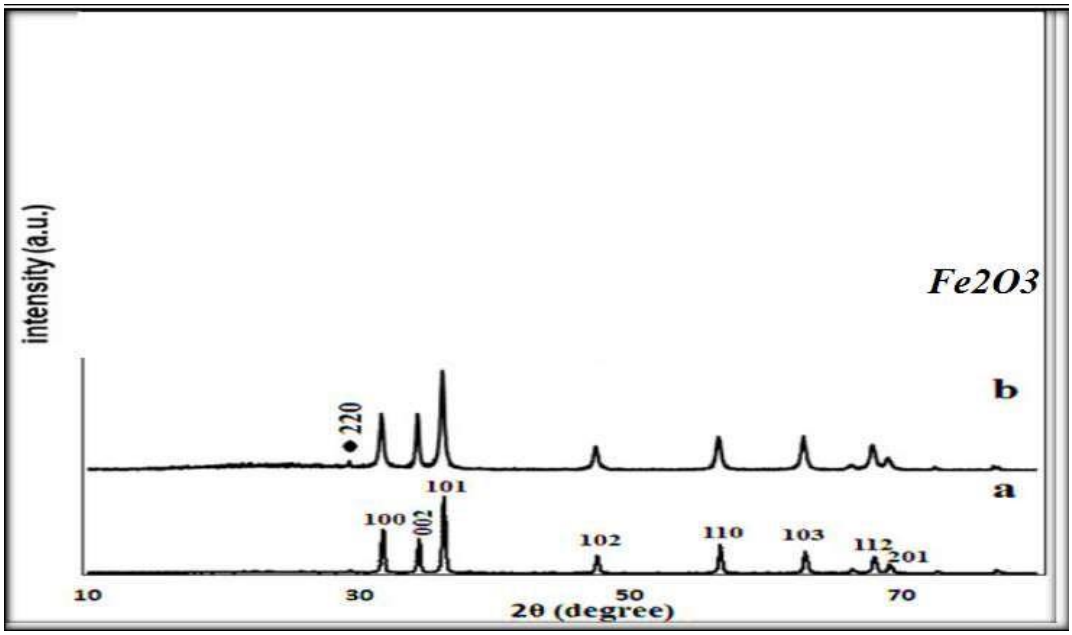

Figure (3): XRD pattern for (a) un doped ZnO and (b) Fe_2O_3 doped ZnO

nanostructures at concentrations 1%.

Figure (4) depicts the EDX spectra of Fe_2O_3 doped ZnO. From this figure, the results prove that the synthesized Fe_2O_3 doped ZnO specimens chiefly contains elements of Zn, C, and O; With a peak of C appears at 0.02 keV, O peak appears at 0.5 keV, and Fe at 0.7 keV and 6.4 keV while Zn appears at peaks of 9.5 keV, 8.6 keV, and 1 keV. Never traces of other elements are observing in the EDX chart. Thus, EDX results are compatible with the XRD result of Fe_2O_3 doped ZnO specimens.

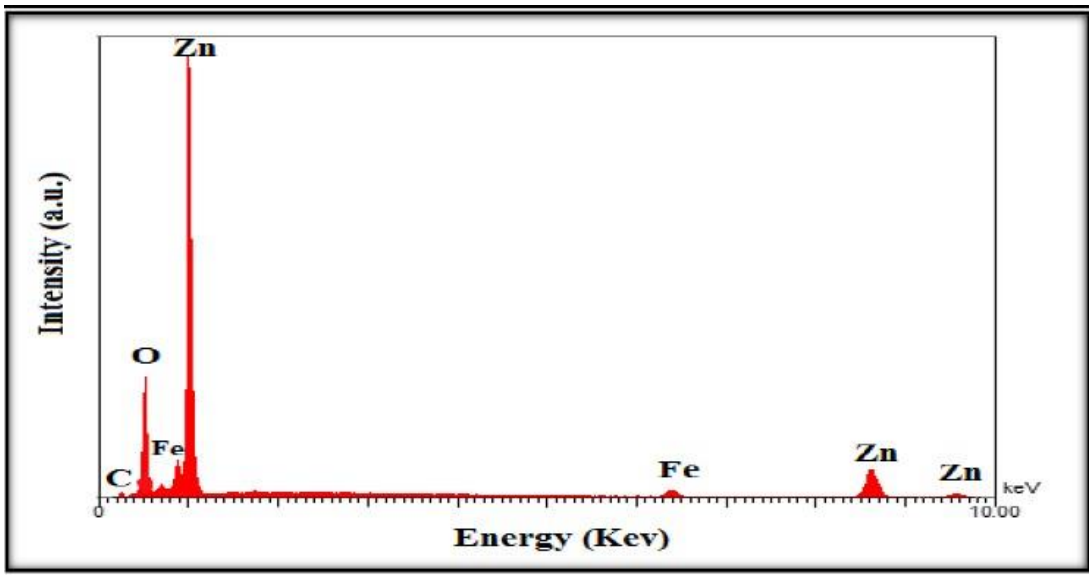

Figure (4): The EDX spectrum of Fe_2O_3 doped ZnO nanostructures

Table (3): XRD results of Fe_2O_3 doped ZnO nanostructures

Prepared conditions	*(2Θ)° XRD*	***I/Io** XRD*	*d(Å) XRD*	*(h k l)*	*FWHM XRD*	*(2Θ)° JCPDS*
1% Fe_2O_3 doped ZnO	31.75	52	2.81563	(100)	0.335	-
	34.40	52	2.60463	(002)	0.274	-
	36.23	100	2.47741	(101)	0.321	-
	47.51	24	1.91188	(102)	1.911	-
	56.56	35	1.62571	(110)	0.382	-
	62.81	33	1.47808	(103)	0.366	-
	67.91	27	1.37908	(112)	0.363	-
	69.03	12	1.35940	(201)	0.360	-
	29.38	4	3.03799	(220)*	0.224	30.09

Table (4): Structural parameters of Fe_2O_3 doped ZnO nanostructures.

Prepared conditions	*(h k l)*	*D (nm)*
Undoped ZnO	(101)	30.1
1% Fe_2O_3 doped ZnO	(101)	26.05

FESEM of doped ZnO:

Field emission scanning electron microscopy (FESEM) provides topographical and elemental information at magnifications of 10x to 300,000x, with virtually unlimited depth of field. Compared with convention scanning electron microscopy (SEM), field emission SEM (FESEM) produces clearer, less electrostatically distorted images.

Ag-doped ZnO nanostructures:

Figure (5) reveals the FESEM images of manufactured ZnO nanostructures. Images (A1, A2) show a rough surface and agglomeration of NPs as a dominant structure with a diameter range of 29.53 nm to 43.46 nm; and images (B1,B2) also show agglomeration of NPs with a diameter range 16 nm to 72.19 nm. Here the difference in both shapes and dimensions of Ag-doped ZnO specimens contributes to the growth of surface area to a volume furthermore activity, which leads to improving the properties.

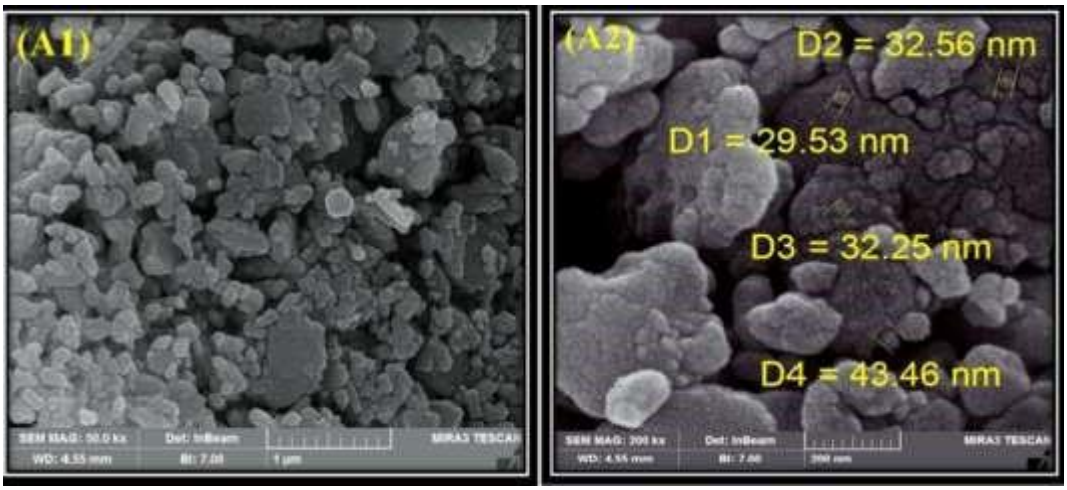

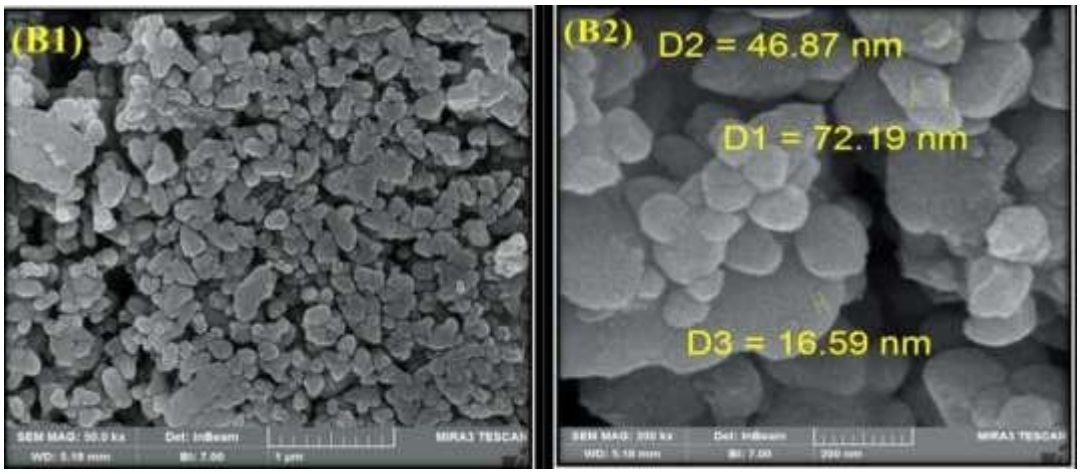

Figure (-5): FESEM images of Ag doped ZnO surface morphologies (A1, A2) of undoped, and doped concentrations (B1, B2) 1%.

Fe_2O_3 doped ZnO nanostructures:

Figure (4-6) exhibits FESEM images of Fe_2O_3 doped ZnO nanostructures surface morphologies. For image (A1, A2) at a doped concentration of 1%, result shows agglomeration of NPs with diameter range 21.26 nm to 26.80 nm. The results show the presence of "thorns or burrs or rock breakers nanostructures" with a small NPs on agglomeration of nanostructures, with the diameter range.

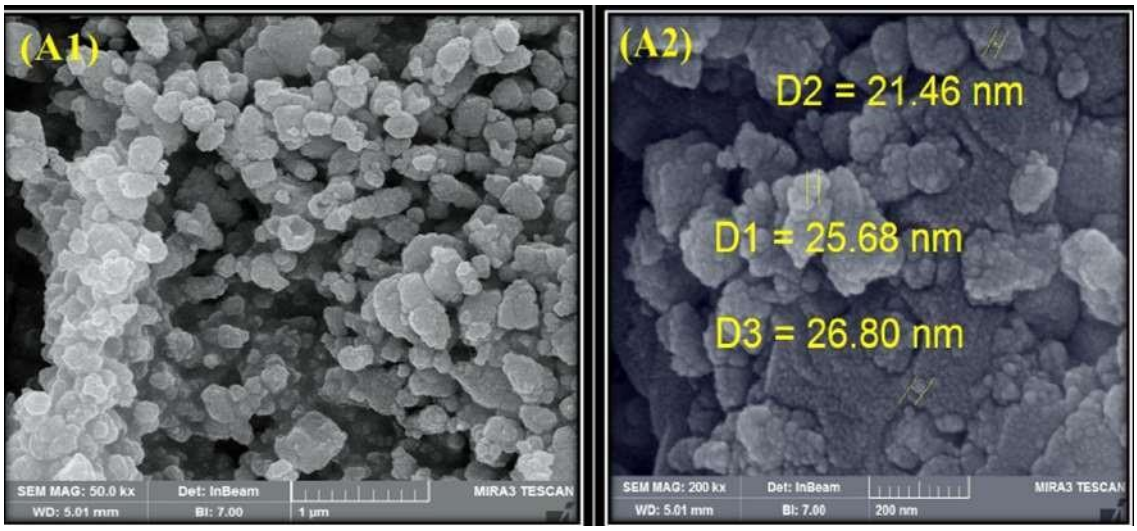

Figure (6): FESEM images of Fe_2O_3 doped ZnO surface morphologies, at doped concentrations (A1,A2) 1%.

Antibacterial Activity of doped ZnO/PVC surfaces:

The antibacterial activity of Zn, Ag and Fe_2O_3 ZnO/PVC surfaces that prepared has been studied, by using THF as solvent and ethanol as non\solvet. The efficiency of anti-bacterial activity is obtained as shown in petri dish and has been measured against four stander bacterial isolates; Gram-positive bacteria staphylococcus-aureus, Gram-positive bacteria (staph. epidermidis), Gram- negative bacteria *E-coli* and Gram-negative bacteria (klebsiella spp.). And also one type of Funguses: Candidiasis.

As shown in the figure (7), the area in which the nanoparticles were injected has a high killing efficiency and is called the inhibition area. It has been observed that the area of inhibition is rather large, relative to the concentration that has been used.

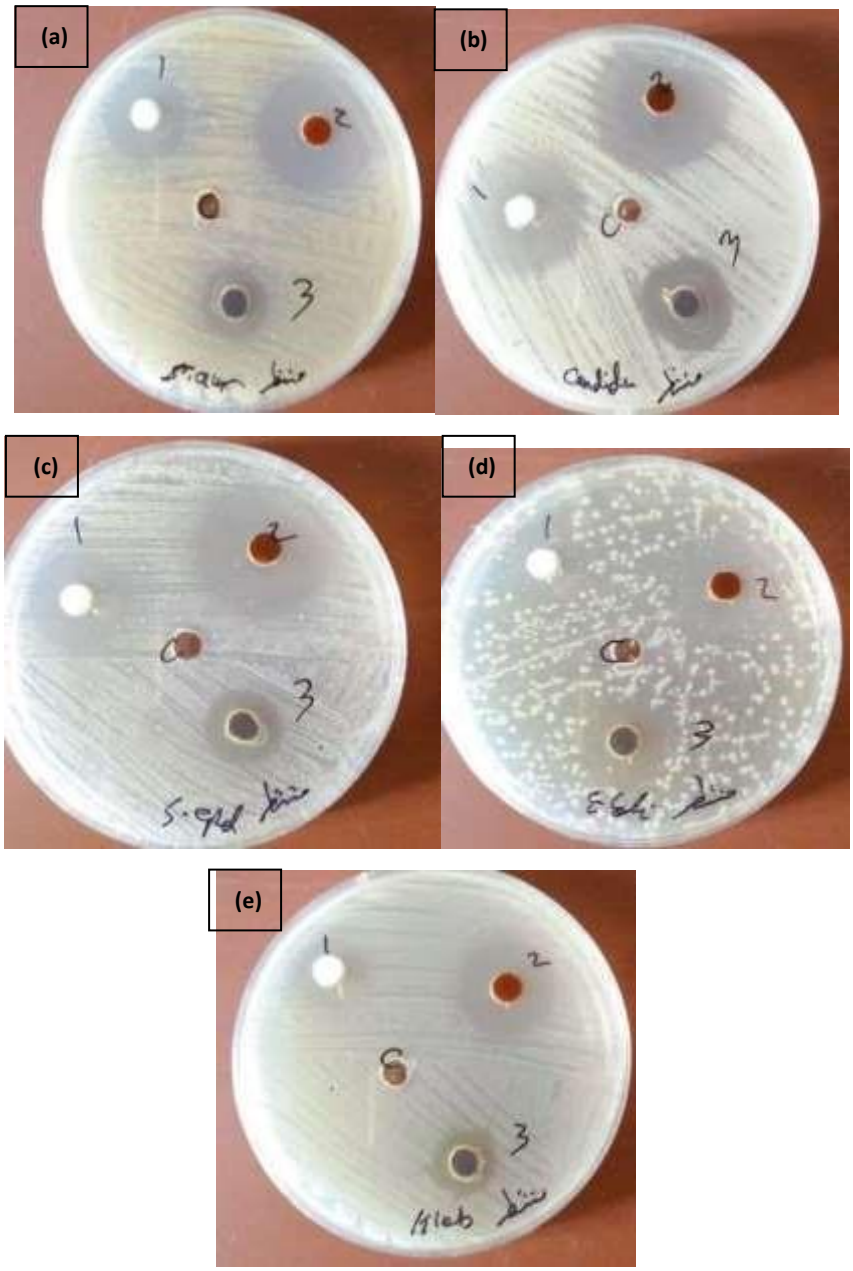

5.Conclusion

1. The structural results show us the XRD pattern of un doped ZnO and Agdoped ZnO nanostructures with higher peak intensities of XRD spectra that are due to the high crystallinity.

2. The surface morphology shows a rough surface and agglomeration of NPs as a dominant structure with a diameter range of 29.53 nm to 43.46 nm.
3. The Antimicrobial Properties shows the activity of nanoparticles for inhibition some types of bacteria. That is why it can be used for the purpose of coating medical devices and this gives the possibility to develop medical devices through the lack of need in the future to sterilize it because it will actually be sterilized.

References

1. M . Raffi, F. Hussain , T . Bhatti , J . Akhter , A . Hameed& M . Hasan
2. (Antibacterial Characterization of Silver Nanoparticles against E: Coli ATCC15224) J. Mater. Sci. Technol., Vol.24 No.2(2008).
3. N.V. Tarasenko, V.S. Burakov, A.V. Butsen (Laser Ablation Plasmas In Liquds For Fabrications Of Nanosize Particles) Publ. Astron. Obs. Belgrade No. 82 (2007).
4. P. J. Thomas (Mesoscopic organization and properties of nanocrystals of metals, metal oxides and other materials) PhD thesis, Bangalore – INDIA (2003).
5. P. Sen, J. Ghosh, A. Abdullah, P. Kumar, Vandana (Preparation of Cu, Ag, Fe and Al nanoparticles by the exploding wire technique) Proc. Indian Acad. Sci. (Chem. Sci.) 115, (2003) 499–508.
6. A. R. Siekkinen, J. M. McLellan, J. Chen, Y. Xia (Rapid synthesis of small silver nanocubes by mediating polyol reduction with a trace amount of sodium sulfide or sodium hydrosulfide) Chemical Physics Letters 432 (2006) 491–496.
7. D. Mirela (MetallicNanoparticles) PhD thesis, (2005).
8. M .Garcia (Corrigendum: Surface plasmons in metallic nanoparticles: fundamentals and applications),J. Phys. D: Appl. Phys. 45(2012) 389501 (1pp). [8] C. Marambio, V. Hoek (A review of the antibacterial effects of silver nanomaterials and potential implications for human health and the environment) J Nanopart Res (2010) 12:1531– 1551. [9] K. Singh, M. Panghal and S. Kadyan,
9. (Green Silver Nanoparticlesas antibacterial Agent), J. Nanobiotechnology, vol. 12, No.40, (2014)
10. K. Singh, M. Panghal and S. Kadyan, (Green Silver Nanoparticlesas antibacterial Agent), J. Nanobiotechnology, vol. 12, No.40, (2014).
11. K. Shameli, M. Bin Ahmed, S. Zayeri (Investigation of antibacterial properties of Silver Nanoparticles prepared via Green Method), Chemistry Central Journal,

12. Vol. 6, No. 73, (2011).

13. Graf C, Vossen DL, Imhof A, van Blaaderen A (July 11, 2003). "A General Method To Coat Colloidal Particles with Silica". Langmuir. 19 (17): 6693–6700.
14. doi:10.1021/la034785

15. Buzea, C., Pacheco, II, and K. Robbie, Nanomaterials and nanoparticles: sources and toxicity. Biointerphases, 2007. 2(4): p. MR17-71

16. Poole Jr, C.P. and F.J. Owens, Introduction to nanotechnology. 2003: John Wiley & Sons.

17. Xia Y, Xiong Y, Lim B, Skrabalak SE (2008). "Shape-controlled synthesis of metal nanocrystals: simple chemistry meets complex physics?". Angewandte Chemie. 48(1): 60–103. doi:10.1002/anie.200802248. PMC 2791829. PMID 19053095.

18. LaMer VK (1950). "Theory, Production and Mechanism of Formation of Monodispersed Hydrosols". Journal of the American Chemical Society. 72 (11): 4847–4854. doi:10.1021/ja01167a001.

19. Kim T, Lee K, Gong MS, Joo SW (October 2005). "Control of gold nanoparticle aggregates by manipulation of interparticle interaction". Langmuir. 21 (21): 9524–8. doi:10.1021/la0504560. PMID 16207031.

20. Ahamed M, Alsalhi MS, Siddiqui MK (December 2010). "Silver nanoparticle applications and human health". Clinica Chimica Acta; International Journal of Clinical Chemistry. 411 (23–24): 1841–8. doi:! 10.1016/j.cca.2010.08.016. PMID 20719239.

21. [18]-Gopinath P, Gogoi SK, Sanpui P, Paul A, Chattopadhyay A, Ghosh SS (June 2010). "Signaling gene cascade in silver nanoparticle induced apoptosis". Colloids and Surfaces. B, Biointerfaces. 77 (2): 240–5. doi:10.1016/j.colsurfb.2010.01.033. PMID 20197232.

22. Lynam C. P., Llope M., Möllmann C., Helaouët P., Bayliss-Brown G. A., & Stenseth N.C. (2017). Interaction between top-down and bottom-up control in marine food webs

23. Bouadma L, Wolff M, Lucet JC (August 2012). "Ventilator-associated pneumonia and its prevention". Current Opinion in Infectious Diseases. 25 (4): 395–404. doi:10.1097/QCO.0b013e328355a835. PMID 22744316. S2CID 41051853.

24. a b Lederer JW, Jarvis WR, Thomas L, Ritter J (2014). "Multicenter cohort study to assess the impact of a silver-alloy and hydrogel-coated urinary catheter on symptomatic catheter-associated urinary tract infections". Journal of Wound, Ostomy, and Continence Nursing. 41 (5): 473–80. doi:10.1097/WON.0000000000000056. PMC 4165476. PMID 24922561.

25. Wasiak J, Cleland H, Campbell F, Spinks A (March 2013). "Dressings for superficial and partial thickness burns". The Cochrane Database of Systematic Reviews. 3 (3): CD002106. doi:10.1002/14651858.CD002106.pub4. PMC 7065523. PMID 23543513.

26. Drugs@FDA. U.S. Food and Drug Administration (FDA). Archived from the original on 2014-09-05. Retrieved 2010-07-10

27. Dissemond J, Böttrich JG, Braunwarth H, Hilt J, Wilken P, Münter KC (May 2017). "Evidence for silver in wound care - meta-analysis of clinical studies from 2000-2015". Journal der Deutschen Dermatologischen Gesellschaft = Journal of the German Society of Dermatology. 15 (5): 524–535. doi:10.1111/ddg.13233.
28. PMID 28485879. S2CID 3752748.

29. Li X, Yuan Q, Wang L, Du L, Deng L (February 2012). "Silver-coated endotracheal tube versus non-coated endotracheal tube for preventing ventilatorassociated pneumonia among adults: a systematic review of randomized controlled trials". Journal of Evidence-Based Medicine. 5 (1): 25–30. doi:10.1111/j.17565391.2012.01165.x. PMID 23528117. S2CID 23720955.

30. Lam TB, Omar MI, Fisher E, Gillies K, MacLennan S (September 2014). "Types of indwelling urethral catheters for short-term catheterisation in hospitalised adults". The Cochrane Database of Systematic Reviews (9): CD004013. doi:10.1002/14651858.CD004013.pub4. PMID 25248140.

31. Anwar A, Rajendran K, Siddiqui R, Raza Shah M, Khan NA (January 2019). "Clinically Approved Drugs against CNS Diseases as Potential Therapeutic Agents To Target Brain-Eating Amoebae". ACS Chemical Neuroscience. 10 (1): 658–666. doi:10.1021/acschemneuro.8b00484. PMID 30346711.

32. Zennaro F, Oliveira Gomes JA, Casalino A, Lonardi M, Starc M, Paoletti P, et al. (2013). "Digital radiology to improve the quality of care in countries with limited resources: a feasibility study from Angola". PLOS ONE. 8(9): e73939.

33. Bibcode:2013PLoSO...873939Z. doi:10.1371/journal.pone.0073939. PMC 3783475. PMID 24086301

34. Last Updated September 2014). National Center for Complementary and Integrative Health. July 2009. Retrieved 9 October 2016

35. Fredrickson JK, Zachara JM, Balkwill DL, Kennedy D, Li SM, Kostandarithes HM, Daly MJ, Romine MF, Brockman FJ (July 2004). "Geomicrobiology of high-level nuclear waste-contaminated vadose sediments at the Hanford site, Washington state". Applied and Environmental Microbiology. 70 (7): 4230–41. doi:10.1128/AEM.70.7.4230-4241.2004. PMC 444790. PMID 15240306.

36. Slonczewski JL, Foster JW (2013). Microbiology : an Evolving Science (Third ed.). New York: W W Norton. p. 82. ISBN 978-0393123678.

37. Susan R. Mikkelsen & Eduardo Cortón. Bioanalytical Chemistry, Ch. 13. Centrifugation Methods. John Wiley & Sons, Mar 4, 2004, pp. 247–267.

38. Basics of Centrifugation". Cole-Parmer. Retrieved 11 March 2012-994.

39. M. Saad Bhamla, Brandon Benson, Chew Chai, Georgios Katsikis, Aanchal Johri & Manu Prakash (10 January 2017). "Hand-powered ultralow-cost paper centrifuge". Nature. 1: 0009. doi:10.1038/s41551-016-0009.

40. Introduction to X-ray diffraction from the University of California, Santa Barbara [broken link].

41. Zhong, Zhang Jin. Optical properties and spectroscopy of nanomaterials. World Scientific, 2009.
42. ACC Esteves, Yuan Luo, MWP Van de Put, CCM Carcouët, G De With Advanced Functional Materials 24 (7), 986-992, 2014.

43. Bhargav, H. S., Shastri, S. D., Poornav, S. P., Darshan, K. M., & Nayak, M.
44. M. (2016, February). Measurement of the Zone of Inhibition of an Antibiotic. In *2016 IEEE 6th International Conference on Advanced Computing (IACC)* (pp. 409-414). IEEE